

## NRC Publications Archive Archives des publications du CNRC

### Further examinations on extinction and bifurcations of radiative CH<sub>4</sub>/air and C<sub>3</sub>H<sub>8</sub>/air premixed flames

Ju, YiGuang; Masuya, Goro; Liu, Fengshan; Guo, Hongsheng; Maruta, Kaoru; Niioka, Takashi

This publication could be one of several versions: author's original, accepted manuscript or the publisher's version. /  
La version de cette publication peut être l'une des suivantes : la version prépublication de l'auteur, la version  
acceptée du manuscrit ou la version de l'éditeur.

For the publisher's version, please access the DOI link below. / Pour consulter la version de l'éditeur, utilisez le lien  
DOI ci-dessous.

#### **Publisher's version / Version de l'éditeur:**

[https://doi.org/10.1016/S0082-0784\(98\)80107-0](https://doi.org/10.1016/S0082-0784(98)80107-0)

*Symposium (International) on Combustion, 27, 2, pp. 2551-2557, 1998*

#### **NRC Publications Archive Record / Notice des Archives des publications du CNRC :**

<https://nrc-publications.canada.ca/eng/view/object/?id=f9d7c8f1-4481-4918-84a0-f18ff15223d2>

<https://publications-cnrc.canada.ca/fra/voir/objet/?id=f9d7c8f1-4481-4918-84a0-f18ff15223d2>

Access and use of this website and the material on it are subject to the Terms and Conditions set forth at

<https://nrc-publications.canada.ca/eng/copyright>

READ THESE TERMS AND CONDITIONS CAREFULLY BEFORE USING THIS WEBSITE.

L'accès à ce site Web et l'utilisation de son contenu sont assujettis aux conditions présentées dans le site

<https://publications-cnrc.canada.ca/fra/droits>

LISEZ CES CONDITIONS ATTENTIVEMENT AVANT D'UTILISER CE SITE WEB.

**Questions?** Contact the NRC Publications Archive team at

PublicationsArchive-ArchivesPublications@nrc-cnrc.gc.ca. If you wish to email the authors directly, please see the  
first page of the publication for their contact information.

**Vous avez des questions?** Nous pouvons vous aider. Pour communiquer directement avec un auteur, consultez la  
première page de la revue dans laquelle son article a été publié afin de trouver ses coordonnées. Si vous n'arrivez  
pas à les repérer, communiquez avec nous à PublicationsArchive-ArchivesPublications@nrc-cnrc.gc.ca.

## FURTHER EXAMINATIONS ON EXTINCTION AND BIFURCATIONS OF RADIATIVE CH<sub>4</sub>/AIR AND C<sub>3</sub>H<sub>8</sub>/AIR PREMIXED FLAMES

YIGUANG JU,<sup>1</sup> GORO MASUYA,<sup>1</sup> FENGSHAN LIU,<sup>2</sup> HONGSHENG GUO,<sup>3</sup> KAORU MARUTA,<sup>4</sup>  
AND TAKASHI NIIOKA<sup>4</sup>

<sup>1</sup>*Dept. of Aeronautics and Space Engineering  
Tohoku University*

*Aramaki Aoba, Aoba-ku, Sendai 980, Japan*

<sup>2</sup>*Combustion Technology, Bldg M-9  
Institute for Chemical Process and Environmental Technology  
National Research Council  
Ottawa, K1A 0R6 Canada*

<sup>3</sup>*Centre for Advanced Gas Combustion Technology  
Dept. of Chemical Engineering  
Queen's University at Kingston  
Ontario, K7J 3N6 Canada*

<sup>4</sup>*Institute of Fluid Science  
Tohoku University  
Katahira 2-1-1, Sendai 980-77, Japan*

The extinction and flame bifurcations of radiative CH<sub>4</sub>/air and C<sub>3</sub>H<sub>8</sub>/air free propagating flames and counterflow flames are investigated numerically with detailed chemistry as well as the optically thin and spectral emission-absorption statistical narrow band models. For counterflow CH<sub>4</sub>/air flame, a G-shaped extinction curve is obtained. It is shown that flame bifurcations and extension of the flammability limit due to the interaction of radiation and stretch at subunity Lewis number exist regardless the radiation model used. Furthermore, it is shown that even for small-scale flame, radiation reabsorption greatly extends the flammable regions of the weak flame (WF) and the near-stagnation flame (NSF). For counterflow C<sub>3</sub>H<sub>8</sub>/air flame, a K-shaped extinction curve is obtained. It is concluded that multiple flame bifurcations are the physically intrinsic phenomena of the practical stretched flames. It is shown that the extrapolation of the stretched extinction limit to zero stretch rate is possible only when the extinction curve is K-shaped. Transition from the G-shaped extinction curve to the K-shaped one, as a result of the competition between radiation heat loss and the Lewis number effect, is examined by replacing the nitrogen gas in CH<sub>4</sub>/air mixture with helium. The critical Lewis number for the transition of the extinction curve is obtained. Results of the present study show good agreement with theory and experiment.

### Introduction

Practical flames are subjected to both radiation heat loss and stretch. It is well known that the standard flammability limit is determined by radiation heat loss [1-6]. Therefore, the study of the extinction and bifurcations of radiative stretched flames is very important for the determination of the standard limit and for the application of the flamelet model to turbulent combustion.

In the experimental measurements of the standard limit and the extinction limit of stretched flames, the spherical propagating flame and the counterflow flame are frequently employed. These flames are subject not only to radiation heat loss but also to stretch effect. Therefore, it is crucial to understand how the measured limits are related to the standard limit (the limit of unstrained flame), and how the combined effect of radiation and stretch affects it.

The study on the combined effects of radiation heat loss and stretch on the extinction of counterflow flame was first investigated numerically by Platt and Tien [7] using a one-step chemistry. Their results showed that there is a radiation-induced extinction at low stretch. Recent microgravity experiments [8] and numerical simulation [9,10] with detailed chemistry obtained a C-shaped extinction curve and demonstrated that radiation heat loss can quench a near-limit flame. Further numerical study [11] and theoretical analysis [12] found that the extinction phenomena are greatly enriched by the interaction of radiation and stretch. This interaction results in multiple flame bifurcations and a G-shaped extinction curve [11] (Fig. 1). This result provided the first successful explanation to the relation between the measured limit and the standard limit.

The study of the Lewis number ( $Le$ ) effect on the

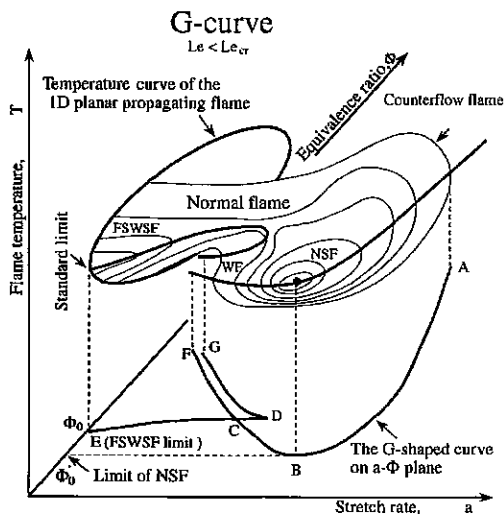


FIG. 1. Schematic illustration of the relation between the flammable region of unstrained flame and counterflow flame for  $Le$  less than a critical value.

flame bifurcation [13] with the one-step chemistry shows that multiple flame bifurcations exist at all the Lewis numbers of practical interests. It is shown that the G-shaped extinction curve changes into a K-shaped curve when the  $Le$  is larger than a critical value. For  $Le$  less than this critical value, a mixture under the standard limit can burn at a moderate stretch. The relation between the flammable region of the unstrained flame and that of the stretched flame for  $Le \leq Le_{cr}$  is shown in Fig. 1. It can be seen that there are four different flame regimes, the sub-limit near-stagnation flame (NSF), near-limit far standing weakly stretched flame (FSWSF), the off-limit normal flame, and the weak flame (WF), for radiative stretched flames. Fig. 1 shows that only the extrapolation of the limit of FSWSF to zero stretch yields the standard limit ( $\Phi_0$ ).

Although many interesting radiation-induced nonlinear phenomena have been revealed in the just-mentioned studies, there are still three questions to be answered. First, the adopted radiation model in the preceding studies is the optically thin approximation. It is well known that  $\text{CO}_2$  and  $\text{H}_2\text{O}$  have strong spectral-dependent radiative properties, and the spectral band absorption coefficients at some bands can be one order higher than the Planck mean absorption coefficient. This implies that radiation reabsorption may be important for near-limit flames even at a very small flame scale. Therefore, it is necessary to know whether flame bifurcations still exist when the spectral emission-absorption is included and how the reabsorption affects the limit. Second, the multibifurcations of  $\text{C}_3\text{H}_8/\text{air}$  flame have not been examined, although a good comparison with

experiment was made in Ref. [10]. Finally, despite the strong nonlinear nature of radiation heat loss, most theoretical analyses employed a linearized treatment as a simplification. Thus, it is important to know how well the theory fits the prediction.

The objective of the present study was to answer the preceding three questions. First, the extinction and bifurcations of the unstrained and stretched  $\text{CH}_4/\text{air}$  flames were examined using both the optically thin and spectral emission-absorption radiation models. The obtained extinction curves were compared with experiment. Then, simulation was carried out for the  $\text{C}_3\text{H}_8/\text{air}$  mixture, and the results were also compared with experiment. Finally, the transition of extinction curve was investigated and compared with theory.

### Physical Model

To compare the limit of a stretched flame with the standard limit, two kinds of flame configurations, the 1-D planar propagating flame (unstrained flame) and the axisymmetrical counterflow premixed flame, were used in this study. A detailed description of the governing equations and the boundary conditions can be found in Ref. [11]. The initial mixture pressure and temperature were respectively 1 atm and 300 K. The downstream length of the burned gas for the unstrained flame was 400 cm. The burner separation for the counterflow flame was fixed at 10 cm.

The fuels considered in this study were  $\text{CH}_4$  and  $\text{C}_3\text{H}_8$ . The Lewis numbers for lean  $\text{CH}_4/\text{air}$  and  $\text{C}_3\text{H}_8/\text{air}$  mixtures are 0.967 and 1.8, respectively. In addition, a  $\text{CH}_4 + [0.21\text{O}_2 + (0.79 - r)\text{N}_2 + r\text{He}]$  ( $0 \leq r \leq 0.79$ ) mixture was also employed to investigate the transition of the extinction curve.  $r$  was varied to change the  $Le$  continuously from 0.967 to 1.8. The C1 chemistry given in Ref. [15] and the C3 chemistry in Ref. [16] were used, respectively, for  $\text{CH}_4$  and  $\text{C}_3\text{H}_8$  flames.

In taking into account the effect of thermal radiation, only the optically thin approximation has been used in previous studies of the standard limit. In this study, both the optically thin model and the statistical narrow band (SNB) model [17] were employed. The band parameters for  $\text{CO}_2$ ,  $\text{H}_2\text{O}$ , and  $\text{CO}$  were taken from Ref. [18]. The radiation transport equations for the SNB model were solved by the discrete ordinate method with the  $T_6$  quadrature scheme [19]. The Planck mean absorption coefficients were taken from Ref. [20] as well as calculated directly from the SNB model in the optically thin limit. Fig. 2 shows a comparison between the predicted Planck mean absorption coefficients of  $\text{H}_2\text{O}$  and  $\text{CO}_2$  with those given in Ref. [20]. It can be seen that the data of Ref. [20] are larger than those obtained from the SNB model. The effect of the Planck mean coefficients on the flammability limit are given in the next

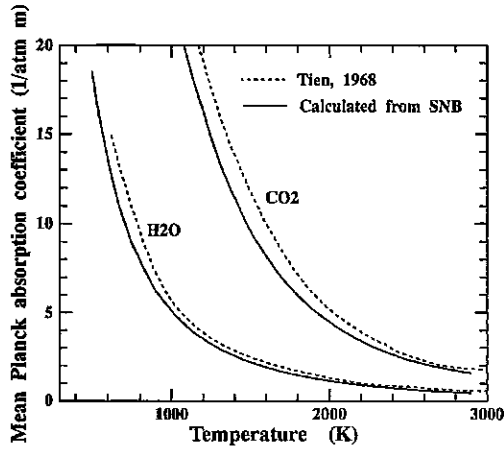


FIG. 2. Comparison of the Planck mean absorption coefficients of CO<sub>2</sub> and H<sub>2</sub>O.

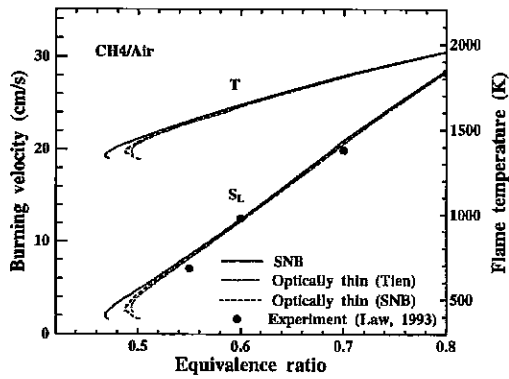


FIG. 3. Burning velocity and flame temperature of an unstrained CH<sub>4</sub>/air flame.

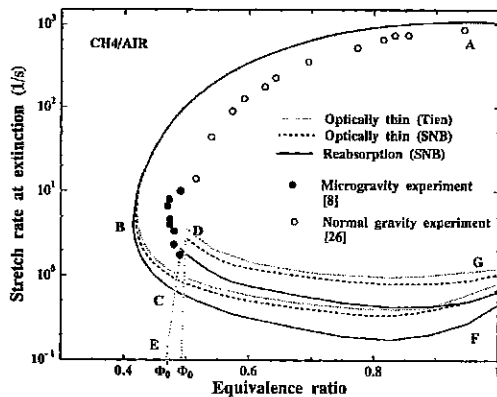


FIG. 4. The effects of the radiation model on the G-shaped extinction curve of a counterflow CH<sub>4</sub>/air flame.

section. Except where noted, the optically thin model used the Planck mean coefficients calculated from the SNB model.

The energy and species conservation equations for both flame configurations were solved by a revised version of the CHEMKIN code [14,15] with the ar-length continuation method [11,21].

## Results and Discussions

### Extinction and Bifurcations of CH<sub>4</sub>/Air Flames

The variation of the burning velocity with equivalence ratio is shown in Fig. 3. The standard flammability limits predicted by the optically thin model using Tien's data [20], the optically thin model using the Planck mean coefficients from the SNB model, and the SNB model, are, respectively, 0.493, 0.488, and 0.468. The flammability limit obtained by Tien's model here agrees exactly with the results in Ref. [22], although a different chemical kinetics was used there. Fig. 3 shows that more accurate radiation models yield a lower standard limit than Tien's model, particularly when radiation reabsorption is taken into account. Therefore, it can be concluded that radiation reabsorption has a great impact on the near-limit flames and the standard limit. A comparison between the predicted data with the experimental data of Ref. [23] shows that the prediction agrees well with the experiment. Although there is a small discrepancy on the lean side, it can be largely attributed to the accuracy of the chemistry. The existing chemical kinetics always gives a larger burning velocity than the microgravity experiment.

The predicted G-shaped extinction curves for a counterflow flame (see Fig. 1) using the preceding three radiation models are shown in Fig. 4. Here, AB is the stretch extinction limit of a normal flame and an NSF (Fig. 1). BC and CF are the radiation extinction limits of the NSF and WF. DG is the jump limit of the WF, and BE is the extinction limit of the FSWSF. Therefore, B represents the flammability limit of the radiative stretched flame, and E is the standard limit of the unstrained flame. Fig. 4 shows that the existence of flame bifurcations is independent of the radiation model used. All the radiation models yield a flammability limit of the stretched flame that is lower than the standard limit. Furthermore, it can be seen that only the extrapolation of the FSWSF limit (DE) to the zero stretch rate yields the standard limit. The comparison between the results obtained using different radiation models reveals that, although flame reabsorption only has a small impact on the flammability limit of the stretched flame, it has a great impact on the radiation limit and the jump limit of the NSF and WF. Therefore, radiation reabsorption is very important for the near-limit and sublimit flames even at a small flame

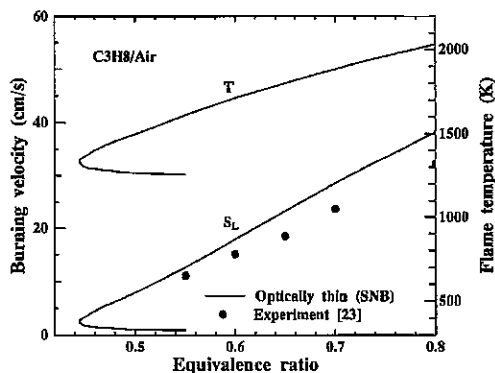


FIG. 5. Burning velocity and flame temperature of an unstrained  $C_3H_8$ /air flame.

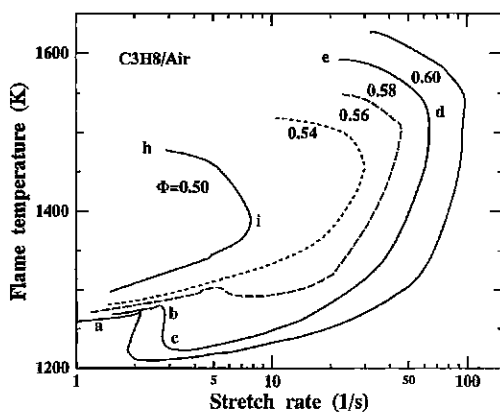


FIG. 6. Relation between flame temperature and stretch rate at typical equivalence ratio.

scale. The microgravity experiment also shows the existence of the radiation limit of the WF. Experimental observation of the FSWSF and the jump limit requires a larger burner separation and a lower stretch rate. Although the SNB model yields a larger discrepancy with the experimental data than the optically thin model, this does not mean that the optically thin model is more accurate. There are two possible reasons for this discrepancy. The main reason is the uncertainty of the chemistry at the lean limit. The other is the limitation of burner diameter used in the microgravity experiment. Therefore, to create a more accurate comparison between prediction and experiment, a further development of chemical kinetics for near-limit flames, and future microgravity experiments with large burner diameters are necessary.

#### Extinction and Bifurcations of $C_3H_8$ /Air Flames

Variation of the burning velocity and flame temperature with the equivalence ratio predicted by the

optically thin model is shown in Fig. 5. It can be seen that the predicted standard flammability limit is 0.445, which is lower than the measured flammability limit of 0.5 [24]. Comparison between prediction and experiment in Ref. [23] also shows that the present chemistry overpredicts the burning velocity. However, this discrepancy becomes smaller as the equivalence ratio decreases.

The flame temperature of the  $C_3H_8$ /air counterflow flame is plotted as a function of the stretch rate in Fig. 6 for typical fuel concentrations. Since the  $Le$  of the lean  $C_3H_8$ /air flame is 1.8, the flow stretch weakens the flame through the  $Le$  effect. On the other hand, the sublimit NSF (Fig. 1) exists because the flame near the stagnation plane suffers less radiation heat loss than the unstrained flame. For  $CH_4$ /air flames, both the  $Le$  effect and the decrease of radiation heat loss due to stretch improve the NSF. Thus, the NSF has a wider flammable region as the  $Le$  goes down. However, the  $Le$  effect for  $Le \geq 1$  plays a counterrole to the radiation effect. Thus, if the  $Le$  effect is stronger than the radiation effect, the sublimit NSF shown in Fig. 1 may not exist.

It can be seen in Fig. 6 that no NSF exists below and above the standard limit. For fuel concentration slightly larger than the standard limit ( $\Phi = 0.5$ ), the FSWSF (hi) appears in the weak stretch region. The minimum separation distance of this flame is 1.2 cm. As the fuel strength further increases, multiflame bifurcations occur at  $\Phi = 0.58$ , where bc is the WF and de is the normal flame. The mechanism of the WF of the  $C_3H_8$ /air flame is similar to that of the  $CH_4$ /air flame [11]. Unlike the lower  $Le$  flame (Fig. 1), the extinction limit of the FSWSF of  $C_3H_8$  flame connects continuously with the stretch extinction limit of the normal flame (cd). This is why the stretch extinction limit of  $C_3H_8$ /air flames can be extrapolated to zero stretch, but that of  $CH_4$ /air flames cannot.

By plotting the stretch extinction limits of the normal flame and FSWSF (d and i) and the radiation extinction limit and jump limit of the WF (b and c) as a function of equivalence ratio, the extinction curve showing the flammable region of all the flame regimes is shown in Fig. 7. It can be seen that the G-shaped extinction curve of  $CH_4$ /air flame became a K-shaped extinction curve. The region below ABC is the flammable region of the normal flame and the FSWSF. The region within the GDF is the coexisting zone of the normal flame and the WF. The K-shaped curve clearly shows that the extrapolation of ABC to zero stretch is the standard limit. Therefore, when the extinction curve is K shaped, the flammability limit of the stretched flame is equal to the standard limit.

The data from microgravity [24] and normal gravity experiments [23] are also shown in Fig. 7. It can be seen that the prediction agrees very well with the experiment. To provide a clear understanding of

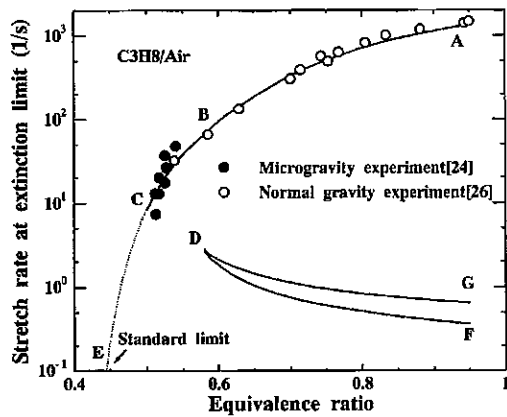


FIG. 7. The K-shaped extinction curve of a counterflow C<sub>3</sub>H<sub>8</sub>/air flame.

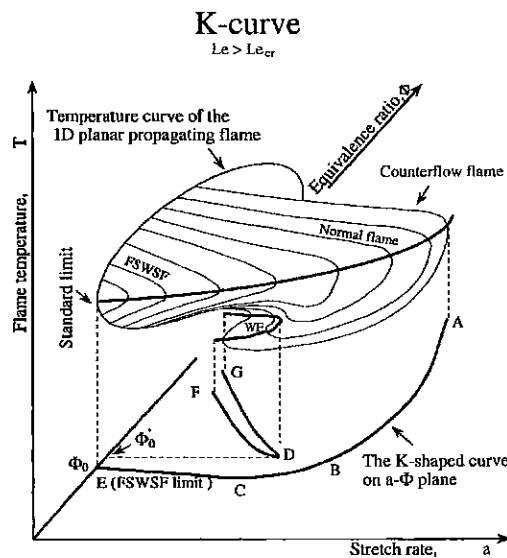


FIG. 8. Schematic illustration of the relation between the flammable region of an unstrained flame and counterflow C<sub>3</sub>H<sub>8</sub>/air flame.

Figs. 6 and 7, the relation of the flammable regions between the unstrained flame and the stretched flame is schematically shown in Fig. 8. Comparison of Fig. 1 with Fig. 8 immediately shows the evolution process from the G-shaped curve to the K-shaped curve.

#### Transition of the Extinction Curve and Comparison with Theory

The preceding results showed that as the  $Le$  increases, the flammability limit of the stretched flame approaches to the standard limit, and the G-shaped

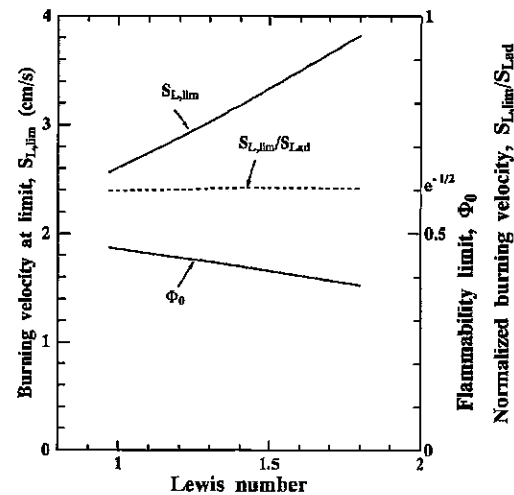


FIG. 9. Dependence of limit burning velocity and standard limit on the  $Le$  of the unstrained CH<sub>4</sub> + [0.21O<sub>2</sub> + (0.79 -  $r$ )N<sub>2</sub> +  $r$ He] flame.

extinction curve reshapes into the K-shaped curve. Therefore, a critical  $Le$  must exist that separates the two distinct extinction curves and at which these two limits become equal.

To examine this transition process, a CH<sub>4</sub> + [0.21O<sub>2</sub> + (0.79 -  $r$ )N<sub>2</sub> +  $r$ He] mixture is used.  $r$  is increased from zero to 0.5 to achieve a continuous change of the  $Le$  from 0.967 to 1.8. For the unstrained flame, theory [3,12,25] shows that the ratio of the radiative flame speed to the adiabatic flame speed at the standard limit is equal to  $e^{-1/2}$ . Fig. 9 shows the burning velocity and the standard limit as a function of the  $Le$ . It can be seen that the standard flammability limit decreases as the  $Le$  increases. There are two mechanisms that affect the limit. The first is the He dilution (increase of  $Le$ ), resulting in a higher flame temperature and thus extending the standard limit. Second, the fast diffusivity of He broadens the thickness of the thermal diffusion zone, leads to larger radiation heat loss, and therefore narrows the flammable region. This can be understood from the limit burning velocity. The burning velocity at the limit increases dramatically as the  $Le$  increases. However, the predicted normalized burning velocity at the limit agrees well with the theoretical value of  $e^{-1/2}$ .

The extinction curves of the stretched flame (the limits of the WF are omitted) at four typical Lewis numbers are shown in Fig. 10. The labeling of each branch is the same as in Fig. 4. It can be clearly seen that the flammability limit (B) of the stretched flame increases as the  $Le$  increases. For  $Le = 1.4$ , the NSF limit (B) becomes larger than the standard limit, and thus the flammability limit of the stretched flame

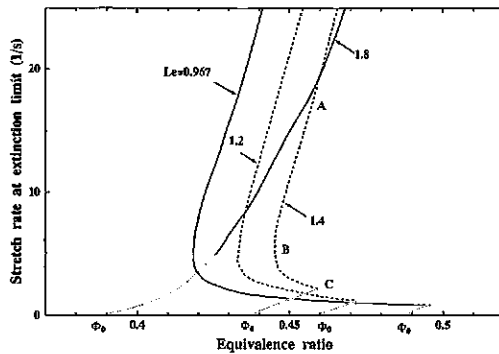


FIG. 10. Extinction curves of the counterflow  $\text{CH}_4 + [0.21\text{O}_2 + (0.79 - r)\text{N}_2 + r\text{He}]$  flame for typical Lewis numbers.

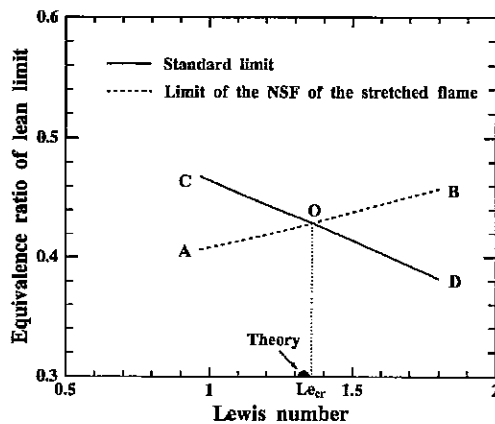


FIG. 11. The flammability limits of unstrained and stretched flames and comparison between prediction and theory on the critical  $Le$ .

becomes equal to the standard limit. Therefore, the critical value will be less than 1.4 (1.36, see Fig. 11).

Theoretical studies in Refs. [3,12,25] have shown the relation between the radiation heat loss and the adiabatic flame temperature at the limit. By comparing these analytical results, a critical  $Le$ , at which the NSF limit and the standard limit becomes equal, can be written as

$$Le_{cr} =$$

$$\left[1 - 2ln(\pi/ln 2)/(1 - T_\infty/T_{ad})(E/RT_{ad})\right]^{-1} \quad (1)$$

Here,  $T_\infty$  and  $T_{ad}$  are, respectively, the ambient temperature and the adiabatic flame temperature at limit.  $E$  and  $r$  are the activation energy and gas constant. For  $\text{CH}_4$  flames,  $E$  is about 43.6 Kcal/mole and  $T_{ad}$  is about 1380 K (Fig. 3). The resulting  $Le_{cr}$  is 1.33.

Figure 11 shows the comparison between the

standard limit and the NSF limit. At  $Le = 1.36$ , the two limits become equal. Thus, 1.36 is the critical  $Le$ . For  $Le$  larger than 1.36, the NSF limit becomes higher than the standard limit, while for  $Le$  less than 1.36, the NSF limit becomes lower than the standard limit. Therefore, line AOD is the flammability limit of the stretched flame. It can be seen that the predicted critical  $Le$  (1.36) agrees very well with the theoretical value (1.33).

## Conclusion

The extinction and bifurcations of stretched and unstrained  $\text{CH}_4/\text{air}$  and  $\text{C}_3\text{H}_8/\text{air}$  flames were studied using detailed chemistry along with the optically thin and SNB radiation models.

It was found that radiation reabsorption greatly enhances the near-limit flame even at a small scale. The results show that radiation limits of both the NSF and the WF are extended by radiation reabsorption. It was confirmed that the existence of the multiple flame bifurcations and four different flame regimes is independent of the choice of radiation model.

It was also found that the G-shaped extinction curve for  $\text{CH}_4/\text{air}$  flames changed into a K-shaped curve for  $\text{C}_3\text{H}_8/\text{air}$  flames. The results show that the stretch extinction limit of a normal flame can be extrapolated to zero-stretch rate only when the extinction curve is K shaped. There is a critical  $Le$  for the transition of the extinction curve. The predicted critical value agrees well with the theory.

The results agree well with available experimental data. However, better comparisons between prediction and experiment require further studies of microgravity experiment and the chemistry, particularly for the near-limit flame.

## REFERENCES

1. Coward, W. F. and Jones, G. W., Bureau of Mines Bulletin 503 (1952).
2. Spalding, D. B., *Proc. Soc. London*, A240:83-100 (1957).
3. Buckmaster, J., *Combust. Flame* 26:151-162 (1976).
4. Lakashima, K. N., Paul, P. J., and Mukunda, H. S., in *Twenty-Third Symposium (International) on Combustion*, The Combustion Institute, 1988, p. 615.
5. Ronney, P. D., *Combust. Flame* 62:121-133 (1985).
6. Sibulkin, M. and Frendi, A., *Combust. Flame* 82:334-345 (1990).
7. Platt, J. A. and Tien, J. S., Chemical and Physical Processes in Combustion, 1990 Fall Technical Meeting, Eastern Section of The Combustion Institute, Orlando, FL, Dec. 3-5, 1990.
8. Maruta, K., Yoshida, M., Ju, Y., and Niioka, T., in *Twenty-sixth Symposium (International) on Combustion*, The Combustion Institute, 1996, p. 1283.

9. Guo, H., Ju, Y., Maruta, K., Niioka, T., and Liu, F., *Combust. Flame* 109:639–646 (1997).
10. Sung, C. J. and Law, C. K., in *Twenty-Sixth Symposium (International) on Combustion*, The Combustion Institute, 1996, p. 865.
11. Ju, Y., Guo, H., Maruta, K., and Liu, F., *J. Fluid Mech.* 342:315–334 (1997).
12. Buckmaster, J., in *Combustion Theory and Modelling*, vol. 1, 1997, pp. 1–11.
13. Ju, Y., Guo, H., Maruta, K., and Niioka T., *Combust. Flame* 113:603–614 (1998).
14. Smooke, M. D., *J. of Comput. Phys.* 48:72–105 (1982).
15. Kee, R. J., et al., Sandia report SAND86-8246.
16. Stahl, G. and Warnatz, J., *Combust. Flame* 85:285–299 (1991).
17. Malkmus, W., Random Lorentz band model with exponential tailed S<sup>-1</sup> line intensity distribution, *J. Opt. Soc. Am.* 57:323–339 (1967).
18. Soufiani, A. and Taine, J., *Int. J. Heat Mass Transfer* 4:987–991 (1997).
19. Liu, F., Gülder, Ö. L., Smallwood, G. J., and Ju, Y., *Int. J. Heat Mass Transfer* 41:2227–2236 (1998).
20. Tien, C. L., *Adv. Heat Transfer* 5:253–323 (1968).
21. Giovangigli, V. and Smooke, M. D., *Combust. Sci. Technol.* 53:23–49 (1987).
22. Law, C. K. and Egolfopoulos, F. N., in *Twenty-Fourth Symposium (International) on Combustion*, The Combustion Institute, 1992, pp. 137–144.
23. Law, C. K., in *Reduced Kinetic Mechanisms for Applications in Combustion System* (N. Peters and B. Rogg, eds.), Springer-Verlag, Tokyo, 1993, pp. 15–26.
24. Maruta, K., Yoshida, M., Kobayashi, H. and Niioka, T., in *Proceedings of Thirty-fourth Japanese Symposium on Combustion*, 1995, p. 414.
25. Joulin, G. and Clavin, P., *Acta Astronautica* 3:223–240 (1976).
26. Law, C. K., Zhu, D. L., and Yu, G., in *Twenty-First Symposium (International) on Combustion*, 1986, p. 1419.

## COMMENTS

*J. P. Gore, Purdue University, USA.* Just as your results show that near-limit flames are affected significantly by reabsorption, they also show that in flames away from extinction, the optically thin limit is a good approximation for opposed flow flames that burn non-sooty fuels with air. In your oral answer, you mentioned that diluents such as CO<sub>2</sub> and SF<sub>6</sub> make reabsorption important. However, it is still important to state that non-sooty fuel/air opposed flow

flames can be treated in optically thin limit, because of wide range of applications in which CO<sub>2</sub>, SF<sub>6</sub> are not used.

*Author's Reply.* Yes, non-sooty fuel/air opposed flow normal flames at large stretch rate can be treated in the optically thin limit. However, when the flame stretch is very low (for example, the weak flame at unity equivalence ratio), the reabsorption will have a significant impact on the flame strength.